Low- and high-temperature electron paramagnetic resonance studies on Cu^{2+}-doped monopyrazine zinc sulphate trihydrate single crystal: observation of the Jahn-Teller effect

1989 J. Phys.: Condens. Matter 1 771

(http://iopscience.iop.org/0953-8984/1/4/010)

J. Phys.: Condens. Matter **1** (1989) 771–781. Printed in the UK

Low- and high-temperature electron paramagnetic resonance studies on Cu^{2+}-doped monopyrazine zinc sulphate trihydrate single crystal: observation of the Jahn–Teller effect

Sushil K Misra and Chunzheng Wang
Physics Department, Concordia University, 1455 de Maisonneuve Boulevard West, Montreal, Quebec, Canada H3G 1M8

Received 15 June 1988, in final form 17 August 1988

Abstract. Electron paramagnetic resonance studies on a single crystal of Cu^{2+}-doped monopyrazine zinc sulphate trihydrate (PZST) have been made over an extended temperature range (4.2–375 K). Three physically equivalent, but magnetically inequivalent, Cu^{2+} complexes have been observed. The spin-Hamiltonian parameters are rigorously evaluated at 334, 295, 77 and 4.2 K, by the method of least-squares fitting, utilising numerical diagonalisation of the spin-Hamiltonian matrix on a digital computer. The principal values of the $\tilde{g}$- and $\tilde{A}$-tensors indicate that, in PZST, the Cu^{2+} ion experiences an octahedral symmetry with orthorhombic distortion. The data are interpreted to conclude the occurrence of both static and dynamic Jahn–Teller effects over the temperature range of investigation, the transition from static to dynamic Jahn–Teller effect occurring at 334 ± 1 K.

1. Introduction

The understanding of the ground states of the Cu^{2+} ion ($3d^9$ electron configuration) in different symmetries of crystal fields is an important topic in electron paramagnetic resonance (EPR). Many studies have been particularly devoted to crystal fields characterised by octahedral symmetry, or octahedral symmetry with a small trigonal distortion, for which the Cu^{2+} ion possesses the twofold-degenerate ground state E_g. Many occurrences of the Jahn–Teller effect (JTE) have been reported in these situations. JTE has been observed by means of EPR in many zinc salts doped by Cu^{2+} ions, e.g. in zinc Tutton salts (Silver *et al* 1974, Petrashen *et al* 1980), zinc fluorosilicate hexahydrate (Bleaney and Ingram 1950), zinc fluorotitanante hexahydrate (De *et al* 1984), zinc bromate hexahydrate (Jesion *et al* 1976, 1977), hexaimidazole zinc dichloride tetrahydrate (Keijzers *et al* 1983) and $K_2Zn(ZrF_6)_2 \cdot 6H_2O$ (Petrashen *et al* 1978). The occurrence of JTE in such cases can be explained as follows. Most cases of JTE for Cu^{2+} are found to occur in diamagnetic host lattices. The diamagnetic ions possess a closed outer electronic shell, thereby causing the local symmetry of the host lattice to be high. When the paramagnetic Cu^{2+} ion is introduced into the diamagnetic host lattice, substituting for the diamagnetic ions, some local distortions are introduced because its size is different from that of the host ions, as well as being paramagnetic. This fulfils the two conditions necessary for the occurrence of JTE (Callaway 1976); namely, that the Cu^{2+} ion be in a

0953-8984/89/040771 + 11 $02.50

degenerate electronic state, and that it occupy a minimum-energy non-degenerate state consequent to the small local distortion of the lattice that it produces.

EPR study of Cu^{2+}-doped monopyrazine zinc sulphate trihydrate, $Zn(C_4H_4N_2)SO_4 \cdot 3H_2O$ (hereafter PZST), has been previously reported by Krishnan (1978), at 295 K on a single-crystal specimen and at 77 K on a polycrystalline specimen. His EPR spectra revealed the existence of three magnetically different sites for Cu^{2+}, although there is only one substitutional position available for Cu^{2+} in the unit cell of PZST. Krishnan explained this to be due to the presence of three domains. He suggested the occurrence of a static JTE in Cu^{2+}-doped PZST from the features of the EPR spectra; the orthorhombic g-values revealed that the admixture of the $|3Z^2 - r^2\rangle$ orbital into the $|X^2 - Y^2\rangle$ orbital was less than 5%.

It is the purpose of this paper to present more detailed EPR studies on Cu^{2+}-doped PZST single crystal. The occurrence of JTE in this low-symmetry crystal is deduced by studying the features of the temperature-dependent EPR spectra. The measurements are carried out over an extended temperature range (4.2–375 K), making it possible to observe a dynamic JTE at high temperatures and a static JTE at lower temperatures. The Cu^{2+} spin-Hamiltonian parameters are evaluated using a rigorous least-squares fitting procedure (Misra 1986, 1988a, b).

2. Sample preparation and crystal structure

Cu^{2+}-doped single crystals were grown by slow evaporation of an aqueous solution, consisting of stoichiometric amounts of pyrazine ($C_4H_4N_2$) and $ZnSO_4 \cdot 7H_2O$, to which was added a sufficient quantity of $CuSO_4 \cdot 5H_2O$ so that there is one Cu^{2+} ion for every 100 Zn ions. The grown crystal possessed the same form as that of the crystal that was used for EPR measurements by Krishnan (1978). It looks like a parallelepiped. The crystal structure of PZST has been reported by Tenhunen (1972) to be triclinic (space group P1); the unit-cell dimensions are $a = 10.734$ Å, $b = 4.427$ Å, $c = 6.927$ Å, $\alpha = 121.15°$, $\beta = 82.57°$, $\gamma = 104.02°$. There is one formula per unit cell ($Z = 1$).

So far, no structure-analysis data have provided the exact positions of Zn^{2+} ions in the lattice of PZST crystal. That the water molecules are not structural water can be concluded from experimental data: the infrared spectrum of PZST reveals that there is no band that confirms water coordination in PZST (Fujita *et al* 1956). In addition, the thermogravimetric curve (Panlik and Erdey 1957) indicates that the three water molecules of PZST are rapidly removed at 115 °C.

3. Experimental arrangement and EPR data

The EPR spectra were recorded on a homodyne X-band Varian V4502 spectrometer, using a 100 kHz field modulation for room- and higher-temperature measurements, and 400 Hz field modulation for measurements at liquid-nitrogen and liquid-helium temperatures. The magnetic-field measurements were made with a Bruker (B-NM20) gaussmeter. The temperature was varied by the use of a heater resistor inside the liquid-helium cryostat for low-temperature measurements. For high-temperature measurements, a Varian variable-temperature controller (model No E4540), attached to a microprocessor digital thermometer, manufactured by Omega (model No 870), was employed.

The angular variation of the data was observed for the Zeeman field ($\boldsymbol{H}$) orientation in three mutually perpendicular planes at every temperature of measurement. The spectra were recorded for the orientation of $\boldsymbol{H}$ at every 4° interval at room and higher temperatures, and at every 5° interval at liquid-nitrogen and liquid-helium temperatures. The most even face of the single-crystal specimen was chosen to define the ZX plane, the plane that contains the crystallographic c axis. The orientation of g_3, the largest g-value (the direction of $\boldsymbol{H}$ for which the positions of the lines are at the minimum) in this plane, was chosen to be the Z axis. For EPR measurements in the ZY and XY planes the specimen was set so that it could be rotated about the X and Z axes, keeping the external magnetic field direction fixed.

3.1. EPR *spectra at room, liquid-nitrogen and liquid-helium temperatures*

The EPR spectra for Cu^{2+}-doped PZST at liquid-nitrogen and liquid-helium temperatures are not much different from that at room temperature. This can be seen from figure 1,

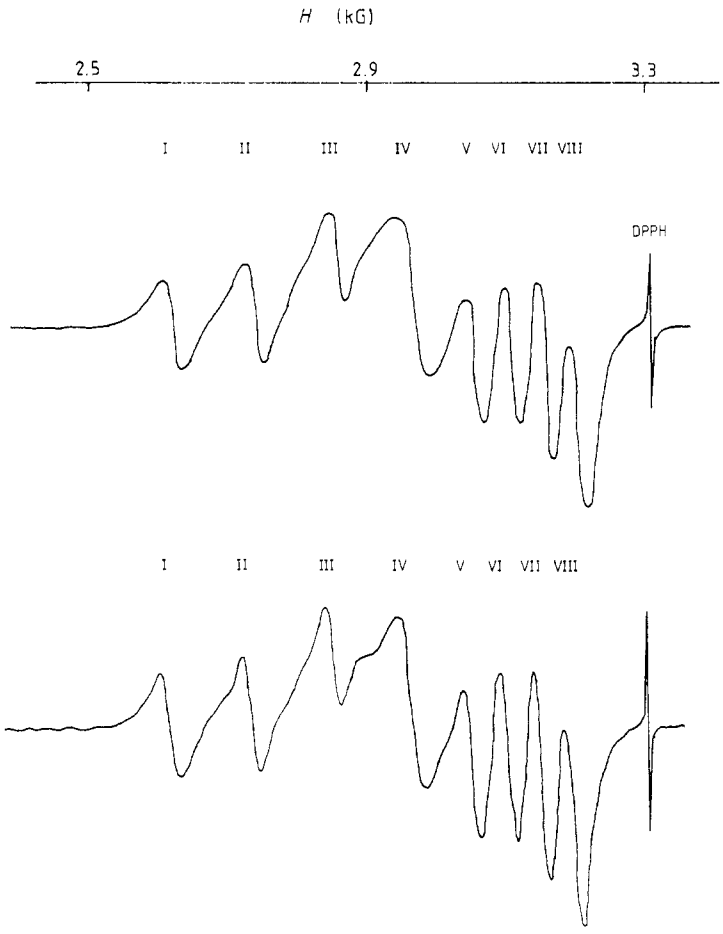

Figure 1. EPR spectra of Cu^{2+}-doped PZST at low temperatures. The upper spectrum is recorded at liquid-nitrogen temperature and the lower one at liquid-helium temperature for $\boldsymbol{H}$ at 75° from the Z axis in the ZY plane.

which exhibits the EPR spectra for the magnetic field orientation at 75° from the Z axis in the ZY plane, at liquid-nitrogen and liquid-helium temperatures. It consists of three sets of four hyperfine (HF) lines, typical of the Cu^{2+} ion; the lines corresponding to the less-abundant isotope of Cu^{2+} (^{65}Cu, 30.91% abundance) could not be clearly seen. The three sets of spectra belong to three physically equivalent, but magnetically inequivalent, Cu^{2+} complexes; thus their angular variations are different, as can be seen from figure 2, exhibiting the angular variations of spectra in the ZY plane at liquid-helium temperature. The line widths do not change significantly, as one lowers the temperature from room to liquid-helium temperature; they are 25, 22, 22, 34, 26, 25, 26 and 21 G, respectively, for the eight clearly resolved EPR lines in increasing order of magnetic field. As can be seen from figure 1, one actually sees only eight clearly resolved lines (indicated as I, II, III, IV, V, VI, VII and VIII). The four lowest-field lines belong to Cu^{2+} ion occupying

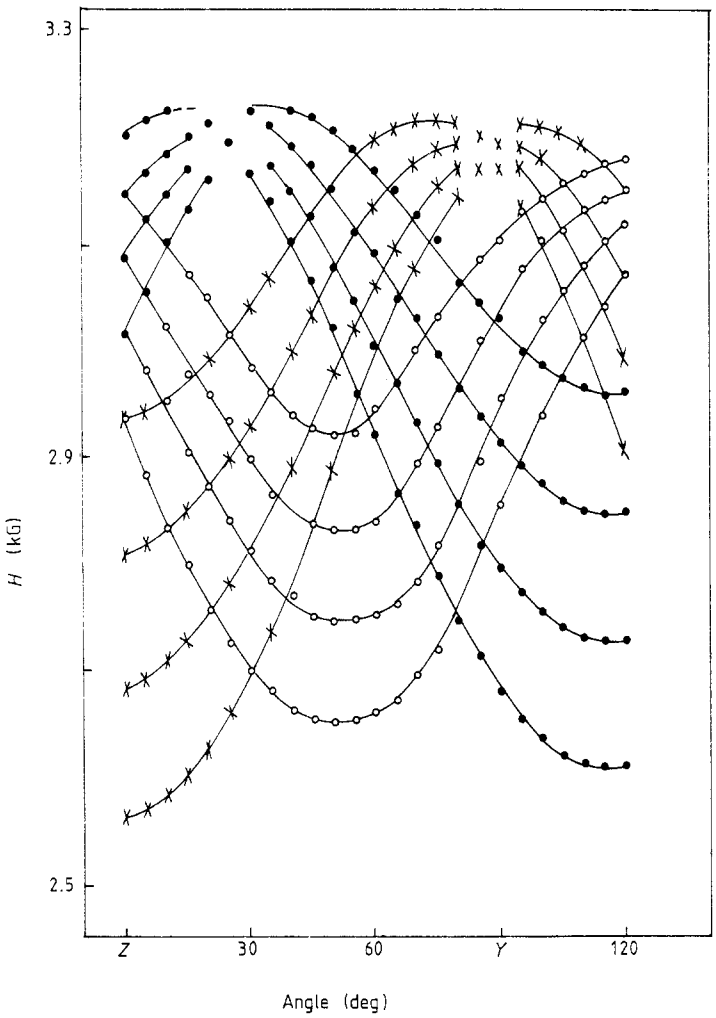

Figure 2. Angular variation of Cu^{2+} EPR spectra in PZST at 4.2 K for the orientation of $\boldsymbol{H}$ in the ZY plane. The full curves connect data points, observed for the same transition. Open circles, full circles and crosses represent three different sets of spectra.

Table 1. The principal values of the $\tilde{g}$- and $\tilde{A}$-tensors (square roots of the principal values of the $\tilde{g}^2$- and $\tilde{A}^2$-tensors, respectively) for Cu^{2+} in PZST at different temperatures. The principal $\tilde{g}$-values are dimensionless, while the principal $\tilde{A}$-values (A_1, A_2, A_3) are in gigahertz. The labelling is such that $g_3 > g_1 > g_2$.

Temperature (K)	g_3	g_1	g_2	A_3	A_1	A_2	Ref.
295	2.3875	2.1924	2.0205	0.324	0.181	0.104	a
295	2.414	2.216	2.109	0.357	0.201	0.132	b
77	2.3876	2.1923	2.0200	0.326	0.182	0.105	a
77	2.42			0.362			c
4.2	2.3868	2.1929	2.0190	0.328	0.185	0.105	a
334	2.191	2.191	2.191				a

[a] Present work.
[b] Krishnan (1978), for a single-crystal specimen.
[c] Krishnan (1978), for a polycrystalline specimen.

site I, the four highest-field lines belong to Cu^{2+} ion occupying site II, while the four lines belonging to Cu^{2+} ion occupying site III overlap the highest-field line of site I and the three lowest-field lines of site II, i.e. overlapping lines IV, V, VI and VII.

The EPR spectra of Cu^{2+} ion in PZST are fitted to the following spin Hamiltonian:

$$\mathcal{H} = \mu_B \boldsymbol{H} \cdot \tilde{\mathbf{g}} \cdot \boldsymbol{S} + \boldsymbol{S} \cdot \tilde{\mathbf{A}} \mathbf{I} \cdot \boldsymbol{I} \tag{1}$$

where μ_B is the Bohr magneton, S ($=\frac{1}{2}$) is the electronic spin and I ($=\frac{3}{2}$) is the nuclear spin of Cu^{2+}.

The principal values of the $\tilde{g}^2$- and $\tilde{A}^2$-tensors and their direction cosines were evaluated by the use of a procedure previously described (Misra 1986, 1988a, b). The principal values of the $\tilde{g}$- and $\tilde{A}$-tensors so evaluated, at various temperatures, are listed in table 1, which also includes the principal values reported by Krishnan (1978). It is

Table 2. Direction cosines of the principal axes of the $\tilde{g}$- and $\tilde{A}$-tensors of Cu^{2+} in PZST. (The same as those of the $\tilde{g}^2$- and $\tilde{A}^2$-tensors respectively.) The direction cosines of the $\tilde{g}^2$-tensor are given with respect to the laboratory axes (X, Y, Z) (as defined in § 3), while those of the $\tilde{A}$-tensor are expressed relative to (X', Y', Z'), the principal axes of the $\tilde{g}^2$-tensor. The values are those found at 295 K.

	Direction cosines of the $\tilde{g}^2$-tensor		
	Z	X	Y
Z'	0.4510	0.2010	0.8696
X'	−0.6486	0.7431	0.1647
Y'	−0.6131	−0.6383	0.4655
	Direction cosines of the $\tilde{A}^2$-tensor		
	Z'	X'	Y'
Z''	0.9999	0.0062	0.0140
X''	−0.0064	0.9998	0.0191
Y''	−0.0103	−0.0192	0.9998

Table 3. Same details as in the caption of table 2. The values are those found at 77 K.

	Direction cosines of the $\tilde{g}^2$-tensor		
	Z	X	Y
Z'	0.4192	0.2720	0.8662
X'	−0.6498	0.7562	0.0770
Y'	−0.6341	−0.5952	0.4937
	Direction cosines of the $\tilde{A}^2$-tensor		
	Z'	X'	Y'
Z''	0.9999	0.0062	0.0100
X''	−0.0064	0.9999	0.0156
Y''	−0.0099	−0.0158	0.9998

noted here that the principal values of the $\tilde{g}$- and $\tilde{A}$-tensors are the same, within experimental error, for the three magnetically inequivalent Cu^{2+} complexes. The direction cosines of the principal axes of the $\tilde{g}$- and $\tilde{A}$-tensors are listed in tables 2–4 at 295, 77 and 4.2 K respectively. (It should be pointed out that the principal values of the $\tilde{g}$- and $\tilde{A}$-tensors are the square roots of the principal values of the $\tilde{g}^2$- and $\tilde{A}^2$-tensors respectively, while the direction cosines of the principal axes of the $\tilde{g}$- and $\tilde{A}$-tensors are the same as those of the $\tilde{g}^2$- and $\tilde{A}^2$-tensors, respectively.)

It is seen from table 1 that the principal values of the $\tilde{g}$- and $\tilde{A}$-tensors remain the same, within experimental error, over the temperature range 77–295 K, while tables 2 and 3 reveal that the principal axes of the $\tilde{g}^2$- and $\tilde{A}^2$-tensors are found to remain coincident over this temperature range. Although the principal values of the $\tilde{g}$- and $\tilde{A}$-tensors at 4.2 K (table 1) are found to be the same as those at room and liquid-nitrogen temperatures, within experimental error, the principal axes of the $\tilde{A}^2$-tensor are no longer coincident with those of the $\tilde{g}^2$-tensor (table 4).

Table 4. Same details as in the caption of table 2. The values are those found at 4.2 K.

	Direction cosines of the $\tilde{g}^2$-tensor		
	Z	X	Y
Z'	0.3649	0.2468	0.8978
X'	−0.6372	0.7692	0.0476
Y'	−0.6788	−0.5895	0.4379
	Direction cosines of the $\tilde{A}^2$-tensor		
	Z'	X'	Y'
Z''	0.9969	0.0788	0.0058
X''	−0.0698	0.9126	−0.4028
Y''	−0.3700	0.4011	0.9153

3.2. EPR spectra above room temperature

Above room temperature, the EPR spectra of Cu^{2+}-doped single crystal of PZST are significantly different from those at room and lower temperatures; the HF lines of Cu^{2+} become broader and weaker. Finally, at 334 ± 1 K, only one single, broad, isotropic line is observed; both the position of the line centre and the line width are independent of the orientation of the external magnetic field. There is no significant change in the line width as the temperature is raised to 375 K, the temperature at which dehydration of the crystal begins to take place. As listed in table 1, this single isotropic line corresponds to $g = 2.191 \simeq (g_1 + g_2 + g_3)/3$, where g_1, g_2 and g_3 are the principal values of the $\tilde{g}$-tensor at room temperature (these values are the same as those below room temperature).

Upon lowering the temperature again below 334 K, after having raised the temperature above 334 K, the features of the EPR spectra return, as observed before. This observation was repeated three times, and each time the features of the EPR spectra were recaptured exactly the same as before recycling through temperatures higher than 334 K. Figure 3 shows the temperature variation of EPR spectra of Cu^{2+}-doped PZST over the range 295–374 K for the external magnetic field orientation at 75° from the Z axis in the ZY plane.

4. Discussion

4.1. Temperatures below 295 K (static JTE)

The principal values of the $\tilde{g}$- and $\tilde{A}$-tensors, over the temperature range 4.2–295 K, as given in table 1, indicate a low symmetry of Cu^{2+} complex in PZST, i.e. orthorhombically distorted octahedral symmetry, since the three principal values, for each of the $\tilde{g}$- or $\tilde{A}$-tensors, are all different from each other. The independence of the EPR spectra, as well as that of the EPR line width, on the temperature below 295 K supports the occurrence of a static JTE, as proposed previously by Krishnan (1978).

The orthorhombic principal g-values due to the static JTE, for any magnetically inequivalent Cu^{2+} complex, as observed presently in PZST, can be analytically expressed as follows (Abragam and Bleaney 1970):

$$\begin{aligned} g_1 &= g_e - (2\lambda/\Delta)[\cos(\varphi/2) + \sqrt{3}\sin(\varphi/2)]^2 \\ g_2 &= g_e - (2\lambda/\Delta)[\cos(\varphi/2) - \sqrt{3}\sin(\varphi/2)]^2 \\ g_3 &= g_e - (8\lambda/\Delta)\cos^2(\varphi/2). \end{aligned} \tag{2}$$

In equations (2) g_e is the g-value of the free electron (=2.0023); λ is the spin–orbit coupling constant for the free Cu^{2+} ion (= $-830\ cm^{-1}$); Δ ($=120B_4^0$) is the octahedral crystal-field splitting constant for Cu^{2+} ion; φ is the vectorial angle of a polar coordinate system (ρ, φ) which describes the distortions Q_ε ($=\rho\sin\varphi$) and Q_θ ($=\rho\cos\varphi$) of the ML_6 complex, where M is Cu^{2+} and L are surrounding ligands, which are not as yet well identified for PZST.

For an arbitrary value of φ (except for $\varphi = n\pi/3$, where n is an integer), the g-values of equations (2) correspond to an orthorhombic distortion of octahedral symmetry (i.e. $g_1 \neq g_2 \neq g_3$), the directions of the principal values g_1, g_2 and g_3 being along the three mutually perpendicular fourfold (tetragonal) axes of the ML_6 complex. The substitutions of the values of $\varphi = \varphi + 2\pi/3$ and $\varphi = \varphi + 4\pi/3$ in equations (2) interchange g_1, g_2 and g_3 amongst themselves, i.e. they correspond to orthorhombic distortions about the

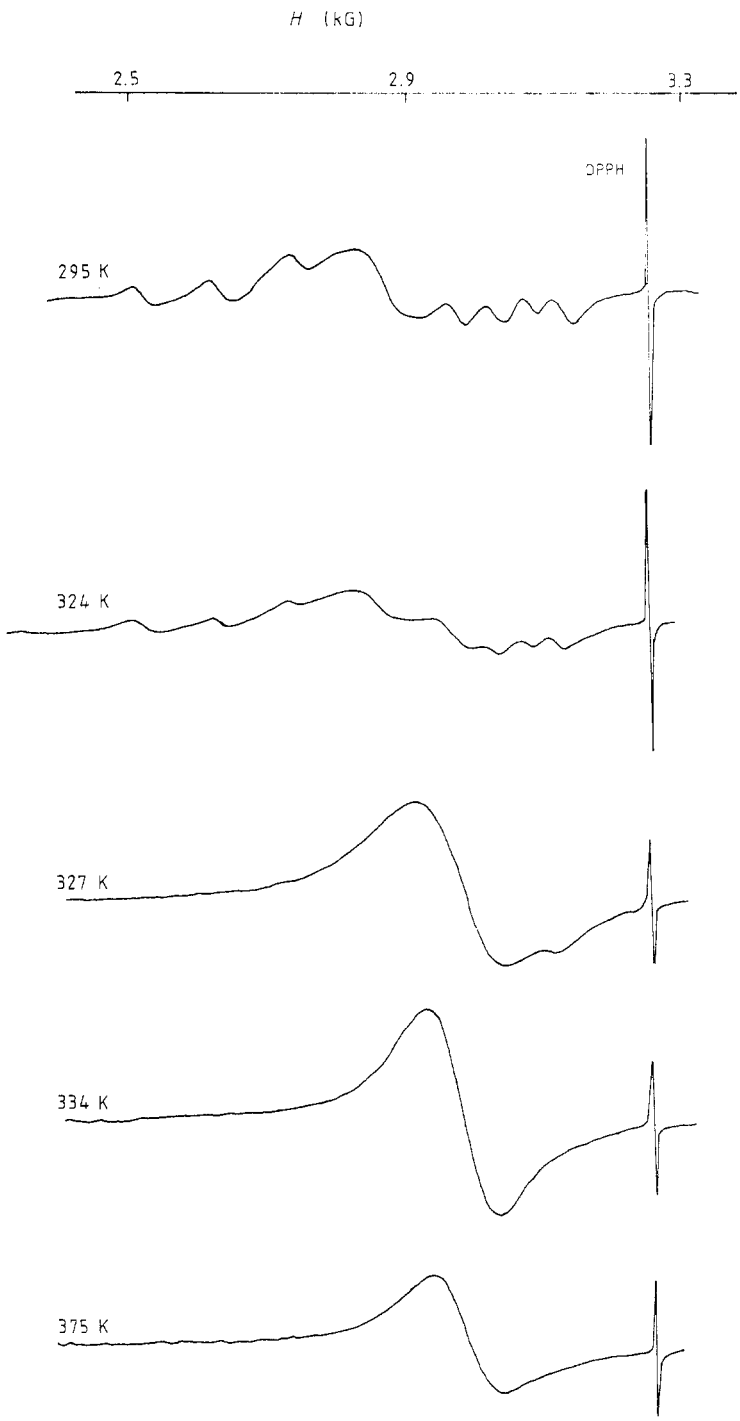

Figure 3. EPR spectra of Cu^{2+}-doped PZST for $\boldsymbol{H}$ at 75° from the Z axis in the ZY plane at 295, 324, 327, 334 and 375 K.

two other tetragonal axes. The potential-energy surfaces, which are associated with the coupling between the magnetic electrons and the ligand nuclei, are referred to as the JT valleys. If φ_0 is the particular value that corresponds to the minimum (i.e. the bottom of the JT valley) of one potential-energy surface, the φ-values corresponding to the minima of the other two potential-energy surfaces are located at $\varphi_0 + 2\pi/3$ and $\varphi_0 + 4\pi/3$. In general, the energies of these three minima are different. In the case of Cu^{2+}-doped PZST, using the typical value of $\lambda/\Delta = -0.05$ (Abragam and Bleaney 1970) in equation (2), and the measured values of g_1, g_2 and g_3, φ_0 has been estimated to be approximately 30°.

Although Krishnan (1978) has ascribed the presence of three sets of EPR spectra at 295 K to the existence of three domains in the crystal, it is entirely possible to account for the present results by supposing that the different JT distortions of the Cu^{2+} complexes (ML_6 type) are randomly distributed with equal probabilities throughout the crystal, rather than grouped into domains. This is further supported by examining the PZST crystal through a polarising microscope, which does not reveal the existence of domains. That such a view naturally leads to a satisfactory explanation of the high-temperature spectrum is presented in § 4.2.

The temperature-dependent principal values $g_i(T)$ and $A_i(T)$ ($i = 1, 2, 3$) can be expressed, in general, as the averages over the three JT potential valleys, with the corresponding weight factors being in proportion to the populations N_1, N_2 and N_3 in the respective JT valleys (Petrashen *et al* 1978). In the case of Cu^{2+}-doped PZST, the principal values of the $\tilde{g}$- and $\tilde{A}$-tensors are found to be independent of temperature in the range 4.2–295 K; this indicates that N_1, N_2 and N_3 are constant, and equal to each other, over the range 4.2–295 K. This is only possible when the energies of the three JT valleys are equal to each other, since the populations in the corresponding JT valleys are governed by a Boltzmann distribution.

Petrashen *et al* (1980) have studied the dynamic JTE nature of $Cu(H_2O)_6^{2+}$ complexes in the zinc and copper Tutton salts, using the EPR and x-ray data. They found that the ratio of the energy splittings between the three JT configurations of the $Cu(H_2O)_6^{2+}$ complex (δ_{13}/δ_{12}), estimated from the temperature-dependent principal values of the $\tilde{g}$-tensor, is close to that estimated taking into account the symmetry of the $Zn(H_2O)_6^{2+}$ complex and the variation of the energy of the JT ion due to the distortions. Thus, the symmetry of the host complex can be deduced from the energy splittings between the three JT valleys of the complex $Cu(H_2O)_6^{2+}$, as determined from EPR data. Proceeding in analogous manner, it is concluded that the energies of the three JT valleys of the Cu^{2+} complex are identical in PZST; the local symmetry of the Zn^{2+} ion in PZST is either regular octahedral or most likely octahedral with a small trigonal distortion. When a Cu^{2+} ion substitutes for a Zn^{2+} ion in PZST, it changes the trigonally distorted octahedral symmetry to orthorhombically distorted octahedral symmetry, because of its different size, and different interaction with ligands. This manifests as static JTE.

The ground state of the Cu^{2+} ion, experiencing an orthorhombic distortion in an octahedral crystal field, is an admixture of $|X^2 - Y^2\rangle$ and $|3Z^2 - r^2\rangle$ orbitals; which one of these two is predominant can be determined from the R-value (Budley and Hathaway 1970), defined to be $R \equiv (g_1 - g_2)/(g_3 - g_1)$, where $g_3 > g_1 > g_2$. When the R-value is greater than unity, a predominantly $|3Z^2 - r^2\rangle$ ground state is expected, while a predominantly $|X^2 - Y^2\rangle$ ground state is expected when it is less than unity. Since the calculated R-value for the present case is less than unity at room temperature and below, the predominant ground state of Cu^{2+} ion, in PZST single crystal, is the $|X^2 - Y^2\rangle$. Further, the admixture of the excited state $|3Z^2 - r^2\rangle$ is given by $\sin^2(\varphi_0/2)$, because the

ground state for Cu^{2+} can be expressed as $\cos(\varphi_0/2)|X^2 - Y^2\rangle + \sin(\varphi_0/2)|3Z^2 - r^2\rangle$ (Abragam and Bleaney 1970). This admixture is less than 7% since $\varphi_0 = 30°$ in the present case, as determined above.

4.2. *Temperatures greater than 295 K (dynamic JTE)*

As the temperature is raised above 295 K, the HF lines of Cu^{2+} become broader through relaxation effects. At $T > 327$ K the HF components become so broad that they are no longer resolved, and only a single isotropic line is observed above 334 K. This is characteristic of a dynamic JTE. This occurs when the rate of tunnelling through the barrier from one distorted configuration of the Cu^{2+} complex (ML_6 type) to the other exceeds the frequency difference between the corresponding EPR resonance lines for the different distorted configurations, i.e. that between the anisotropic spectra (Ham 1972). From the time-averaging effect, when the dynamic JTE occurs, equations (2) yield $g_1 = g_2 = g_3 = g_e - 4\lambda/\Delta$, since the averages $\langle\cos^2(\varphi/2)\rangle = \langle\sin^2(\varphi/2)\rangle = \frac{1}{2}$ and $\langle\cos(\varphi/2)\sin(\varphi/2)\rangle = 0$. From the typical value of $\lambda/\Delta = -0.05$ for Cu^{2+} ion (Abragam and Bleaney 1970), $g_e - 4\lambda/\Delta$ is calculated to be 2.2, very close to the observed g-value (2.191) at $T \geqslant 334$ K. This is characteristic of the type I dynamic JTE (Ham 1972).

Since the EPR spectrum for Cu^{2+} in PZST above 334 K is isotropic as revealed by both the position of the centre of the EPR line and the EPR linewidth, the oriented and random strains are expected to be very small compared to kT, as deduced using the fact that the centre of the EPR line is influenced by the oriented strains, while the EPR line width is influenced by the random strains (Ham 1972).

The observation of only one isotropic line at $T \geqslant 334$ K can be explained to be due to motional averaging, because of rapid hopping between the three equivalent JT-distorted sites, randomly distributed in the crystal with equal probabilities. One then expects a high-temperature 'g'-value of $g = (g_1 + g_2 + g_3)/3 = 2.2$. The observed '$g$'-value of 2.191 is almost equal to 2.2.

5. Concluding remarks

The interpretation of the observed EPR spectra of Cu^{2+}-doped PZST over the temperature range 4.2–375 K has been provided in detail in the present paper. Owing to the extended temperature range (4.2–375 K) over which the EPR measurements were carried out in the present work on a single crystal of PZST, it has been possible not only to study the nature of the EPR spectra at various temperatures but also to confirm the observation of both static and dynamic JTE in Cu^{2+}-doped PZST; the transition between them occurs at 334 ± 1 K. It has been estimated that the heights of the three JT barriers are the same over the range 4.2–295 K.

The present studies lead to the conclusion that the local symmetry of Zn^{2+} site in PZST lattice is most probably octahedral, or octahedral with a small trigonal distortion. This is in contradiction with the suggestion that the coordination around the zinc ion in PZST lattice is tetrahedral (Tenhunen 1972).

The high-temperature EPR spectra are found to be well explained by supposing that the different JT distortions of the Cu^{2+} complex in PZST are randomly distributed with equal probabilities throughout the crystal, rather than being due to the existence of three domains as suggested by Krishnan (1978). This is further supported by the fact that no domains were indeed found upon examination through a polarising microscope.

Acknowledgments

The authors are grateful to the Natural Sciences and Engineering Research Council of Canada for financial support (Grant No A4485), and to the Concordia University Computer Centre for providing their facilities to analyse the data.

References

Abragam A and Bleaney B 1970 *Electron Paramagnetic Resonance of Transition Ions* (Oxford: Clarendon)
Bleaney B and Ingram D J E 1950 *Proc. Phys. Soc.* A **63** 408
Budley R J and Hathaway B J 1970 *J. Chem. Soc.* A 2799
Callaway J 1976 *Quantum Theory of the Solid State* (New York: Academic)
De D K, Rubins R S and Black T D 1984 *Phys. Rev.* B **29** 71
Fujita J, Nakamoto K and Kobayashi M 1956 *J. Am. Chem. Soc.* **78** 3963
Ham F S 1972 *Electron Paramagnetic Resonance* ed. S Geschwind (New York: Plenum) p 54
Jesion A, Shing Y H and Walsh D 1977 *Phys. Rev.* B **16** 3012
Jesion A, Shing Y H, Walsh D and Donnay J D H 1976 *J. Phys. C: Solid State Phys.* **9** L219
Keijzers C P, Jansen T, de Boer E and Van Kalkeren G 1983 *J. Magn. Reson.* **52** 211
Krishnan V G 1978 *J. Phys. C: Solid State Phys.* **11** 3493
Misra S K 1986 *Magn. Reson. Rev.* **10** 285
—— 1988a *Arab. J. Sci. Eng.* **13** 255
—— 1988b *Physica B* **151** 433
Panlik F and Erdey L 1957 *Acta Chim. Acad. Sci.* **13** 117
Petrashen V E, Yablokov Yu V and Davidovich R L 1978 *Phys. Status Solidi* b **88** 439
—— 1980 *Phys. Status Solidi* b **101** 117
Silver B L and Getz D 1974 *J. Chem. Phys.* **61** 638
Tenhunen A 1972 *Acta Chim. Scand.* **22** 1827